Vanadium-Containing Mesoporous Silica of High Photocatalytic Activity and Stability Even in Water

Yasuhiro Shiraishi,* Masatsugu Morishita, Yugo Teshima, and Takayuki Hirai

Research Center for Solar Energy Chemistry, and Division of Chemical Engineering, Graduate School of Engineering Science, Osaka University, Toyonaka 560-8531, Japan

Received: November 16, 2005; In Final Form: February 15, 2006

Vanadium-containing mesoporous silica molecular sieve (V∝HMS) with tetrahedrally coordinated V-oxide species (V^VO_4) has been prepared by a modified surfactant-templating method, consisting of an addition of surfactant to a mixture of water, alcohol, and Si and V precursors followed by calcination. The V∝HMS demonstrates high photocatalytic activity even in the presence of water, while other V∝HMS's prepared by conventional templating methods and V/HMS prepared by an impregnation method show almost no activity owing to hydrolysis of the V^VO_4 species. ESR and photoluminescence measurements reveal that the modified templating method creates V^VO_4 species confined within a silica layer, while other methods create V^VO_4 species exposed on silica surface. The former V^VO_4 species are highly stabilized by the confinement within the silica, thus suppressing the hydrolysis. Another notable property of the confined V^VO_4 species is the higher photocatalytic activity even without water, despite their confined structure. This is explained by higher electrophilicity and longer lifetime of the excited-state V^VO_4 species ($V^{IV}O_4$*) derived from their distorted structure. The obtained findings suggest potential use of the modified surfactant-templating method for synthesis of stable and recyclable V-containing mesoporous silica with high photocatalytic activity.

1. Introduction

Development of efficient photocatalytic systems, driven by a stable and recyclable heterogeneous catalyst, is one of the biggest challenges in chemistry. Recently, transition metal oxides, which are highly dispersed on inorganic support, have received a great deal of attention because these species demonstrate photocatalytic activities that are quite different from those of bulk oxides.[1−4] Among them, highly dispersed vanadium-oxide (V-oxide) species have been studied extensively.[5−7] On the catalyst with low V content, these species exist in a tetrahedral coordination (V^VO_4 species), as shown in Scheme 1, while the catalyst with high V content contains aggregated V_2O_5 clusters. Photoactivated V^VO_4 species promote several unique photocatalytic reactions: V-loaded SiO_2 (V/SiO_2) and Al_2O_3 (V/Al_2O_3) promote partial oxidation of alkanes[8,9] and alkenes[10−12] with molecular oxygen (O_2); hydrothermally synthesized V silicalite with a MEL structure (VS-2) and V-containing mesoporous silica molecular sieve (V∝HMS) promotes NO decomposition and isomerization of olefin.[13,14] The V^VO_4 species are, however, very sensitive to moisture;[15−19] the presence of H_2O in the catalytic system leads to a significant decrease in the catalytic activity and also hydrolysis of the species, resulting in V leaching from the catalyst. Development of catalysts containing "water-resistant" V^VO_4 species, which do not show a decrease in catalytic activity and collapse of the species in the presence of water, is now the focus of attention.

One of the most important catalyst structures required for high catalytic performance is a large surface area, which is achieved by constructing a mesoporous (HMS) structure. V-containing HMS is prepared by a conventional impregnation method (V/HMS),[4] consisting of an addition of silicious HMS to water containing a V precursor (adsorption of the precursor) followed by calcination of the resulting HMS, and by a conventional surfactant-templating method (V∝HMS),[18,20] consisting of hydrolysis of Si and V precursors in the presence of surfactant followed by calcination of the resulting gel. For V∝HMS, two preparation methods have been proposed so far: (i) addition of Si precursor to a mixture of water, alcohol, V precursor, and surfactant (dodecylamine: DA) followed by calcination (V∝HMS-A);[20] and (ii) addition of DA and water to a mixture of alcohol, and Si and V precursors (V∝HMS-B).[18] Herein, we report that a slight modification of these conventional templating methods, consisting of an addition of DA to a mixture of water, alcohol, and Si and V precursors followed by calcination (V∝HMS-C), creates "water-resistant" V^VO_4 species. This catalyst demonstrates high photocatalytic activity even in the presence of water, while V/HMS, V∝HMS-A, and V∝HMS-B catalysts show almost no activity with water. We also found that the V^VO_4 species on V∝HMS-C demonstrates very high photocatalytic activity even in the absence of

SCHEME 1

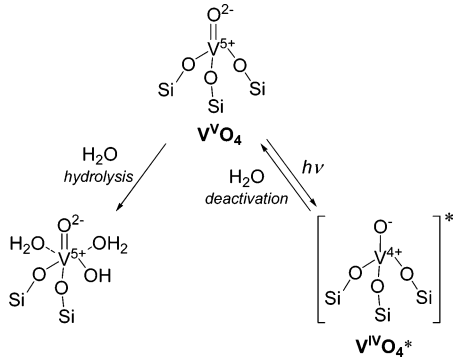

* To whom correspondence should be addressed. E-mail: shiraish@cheng.es.osaka-u.ac.jp. Fax: +81-6-6850-6273. Tel.: +81-6-6850-6271.

10.1021/jp056624e CCC: $33.50
Published on Web 03/14/2006

TABLE 1: Properties of Catalysts and Results of Photocatalytic Oxidation of Cyclohexane[a,b]

					yield (μmol)		
catalyst	V[c] (mol %)	S_A[d] ($m^2\ g^{-1}$)	D_p[e] (nm)	H_2O added (mmol)	cyclohexanone	cyclohexanol	CO_2
V/HMS	1.5	745	2.63	0	8.3	5.4	0.33
				2.8	1.0	0.7	0.01
V∝HMS-A	1.6	886	2.87	0	7.3	6.9	0.15
				2.8	ND	ND	ND
V∝HMS-B	1.5	817	2.63	0	7.5	6.2	0.47
				2.8	ND	ND	ND
V∝HMS-C	1.5	774	2.87	0	13.3	13.0	0.68
				2.8	10.3	10.9	0.48
V_2O_5				0	ND	ND	ND
TiO_2 (P25)				0	146.2	44.8	7.0

[a] Reaction conditions: catalyst, 50 mg; acetonitrile, 9 mL; cyclohexane, 1 mL; O_2, 1 atm; photoirradiation time, 5 h ($\lambda > 300$ nm). [b] ND means "not detected". [c] V/(V + Si) × 100, determined by a dissolution of the catalysts with hydrofluoric acid followed by ICP-AES analysis. [d] BET surface area. [e] Average pore diameter.

water. The properties and structure of the V^VO_4 species have been examined in detail by means of ESR and steady-state and time-resolved photoluminescence measurements. We emphasize here that V^VO_4 species "confined" within a silica layer are the key to high photocatalytic activity and stability against water.

2. Experimental Section

2.1. Materials. All of the reagents used were of the highest commercial quality, which were supplied from Wako Pure Chemical Industries, Ltd., and Tokyo Kasei Co., Ltd., and used without further purification. Water was purified by the Milli Q system. Silicious HMS was synthesized according to literature procedure.[20] V-containing HMS catalysts were prepared as follows. **V/HMS**:[4] NH_4VO_3 (0.01 g) dissolved in water (200 g) was stirred with HMS (0.5 g) at 353 K for 12 h. The resulting HMS was dried at 363 K for 24 h and calcined at 773 K for 5 h under air flow, affording white powder. **V∝HMS-A**:[20] DA (1.85 g) dissolved in ethanol (13.9 g) was added to water (135.2 g) containing Na_3VO_4 (0.013 g), and the solution was stirred at 298 K for 1 h. Tetraethyl orthosilicate (TEOS, 10.4 g) was added slowly to the solution and stirred for 24 h. The solid formed was recovered, washed with water, dried at 373 K for 6 h, and finally calcined at 823 K for 8 h under air flow, affording white powder. **V∝HMS-B**:[18] A mixture of $VOSO_4$ (0.04 g), ethanol (29.9 g), TEOS (20.8 g), and 2-propanol (6.01 g) was stirred for 30 min (solution 1). A mixture of DA (5.00 g), water (67.5 g), and HCl (0.20 g) was stirred for 5 min (solution 2). Both solutions were combined quickly and stirred at 298 K for 18 h. The solid formed was recovered, washed with water, dried at 353 K for 12 h, and finally calcined at 773 K for 6 h under air flow, affording white powder. **V∝HMS-C**: water (135.2 g) and ethanol (13.9 g) were added to a mixture of Na_3VO_4 (0.013 g) and TEOS (10.4 g) with stirring. Immediately, DA (1.85 g) was added dropwise to the mixture and stirred for 24 h at 298 K. The solid formed was recovered, washed with water, dried at 373 K for 6 h, and finally calcined at 823 K for 8 h under air flow, affording white powder. The properties of these catalysts are summarized in Table 1.

2.2. Photoreaction Procedure. Each catalyst (50 mg) was suspended in a mixture of acetonitrile (9 mL) and cyclohexane (1 mL) within a Pyrex glass tube (20 cm^3; ϕ 10 mm), and each tube was sealed using a rubber septum cap. O_2 was bubbled through the solution for 5 min at 273 K to avoid the evaporation of solvent and substrate. The samples were photoirradiated by a Xe lamp (2 kW; Ushio Inc.)[21] at wavelengths of $\lambda > 300$ nm with magnetic stirring, where the light intensity at 300−400 nm was 9.9 mW m^{-2}. The temperature of the solution during photoirradiation was 313 K. After the reaction, the solution was recovered by centrifugation, and the concentrations of the products were determined by GC-FID (Shimadzu; GC-1700) and GC-TCD (Shimadzu; GC-8A), where the product identifications were made by GC-MS (Shimadzu; GCMS-QP5050A).

2.3. ESR Measurement. ESR spectra were recorded at the X-band using a Bruker EMX-10/12 spectrometer with a 100 kHz magnetic field modulation at a microwave power level of 1.0 mW,[22−24] where the microwave power saturation of the signals does not occur. The magnetic field was calibrated using a 1,1′-diphenyl-2-picrylhydrazyl (DPPH) as standard. Photoirradiation of the sample was made using a 500 W Xe lamp (USHIO Inc.; $\lambda > 300$ nm). Each catalyst (100 mg) was placed in a cylindrical quartz ESR tube (capacity, 6 cm^3) and treated with 100 Torr O_2 (1 Torr = 133.3 Pa) at 673 K for 1 h. The tube was evacuated at 673 K for 2 h and cooled to room temperature. H_2, O_2, or cyclohexane (1 Torr) was introduced to the tube. The tube was placed on an ESR sample cavity and photoirradiated at 77 K using a 500 W Xe lamp (USHIO Inc.). After photoirradiation for 0.5 h, measurement was started with continued photoirradiation.

2.4. Other Analyses. Steady-state and time-resolved photoluminescence spectra were recorded using an Hitachi F-4500 fluorescence spectrometer.[25,26] The measurement was carried out as follows: each catalyst (100 mg) was placed in a cylindrical quartz tube (capacity, 6 cm^3) and treated with 75 Torr O_2 at 673 K for 1 h. The tube was evacuated at 673 K for 2 h and cooled to room temperature. Measurement was then carried out at 77 K. After the measurement, the tube was ejected from the sample holder and warmed to room temperature in vacuo. H_2O or cyclohexane (1 Torr) was introduced to the tube, and measurement was made again at 77 K. Total V content of the catalyst was determined by an inductively coupled argon plasma atomic emission spectrophotometer (Nippon Jarrell-Ash.; ICP-AES; ICAP575 Mark II). BET surface area and pore size distribution of the catalysts were determined by N_2 adsorption−desorption measurement at 77 K using a BELSORP 18PLUS-SP analyzer (BEL Japan, Inc.). Diffuse reflectance UV−vis spectra of the catalysts were measured on a UV−vis spectrophotometer (Jasco Corp.; V-550 with Integrated Sphere Apparatus ISV-469) using $BaSO_4$ as reference. Raman spectra were recorded on a Jasco NRS-3100T ($\lambda_{ex} = 532.19$ nm; laser power, 8.4 mW). IR spectra were measured using an FT-IR-610 infrared spectrophotometer (Jasco Corp.).

3. Results and Discussion

3.1. Properties and Activities of Catalysts. Table 1 summarizes the properties of V∝HMS-A, -B, and -C and V/HMS catalysts: all four catalysts show similar V content (1.5−1.6 mol %) and BET surface area (740−890 $m^2\ g^{-1}$). Powder XRD patterns (Figure 1) and N_2 adsorption−desorption isotherms (Figure 2) demonstrate that all of the catalysts have a HMS structure with 2.5−3 nm mesopores. As shown in Figures 3b−3e, Raman spectra of these catalysts show distinctive shifts attributable to Si−O and Si−O−Si groups,[27] whereas shifts at 987, 692, and 519 cm^{-1} attributable to aggregated V_2O_5 cluster do not appear.[28−31] These indicate that these catalysts consist predominantly of highly dispersed (monomeric) V-oxide species. Figure 4 shows diffuse-reflectance UV−vis spectra of the catalysts. All four catalysts, when dehydrated in vacuo at 673 K for 2 h, demonstrate distinctive absorption at <400 nm (solid line), indicating that these contain tetrahedrally coordinated V^VO_4 species (Scheme 1).[28−31]

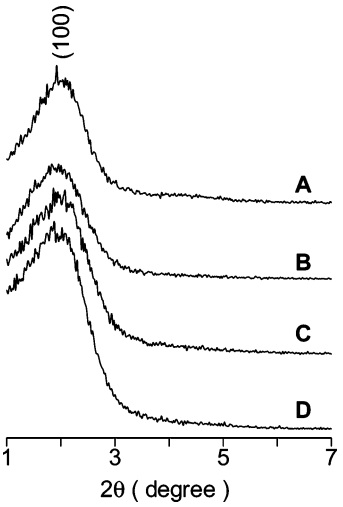

Figure 1. Powder XRD pattern of (A) V∝HMS-A, (B) V∝HMS-B, (C) V∝HMS-C, and (D) V/HMS catalysts.

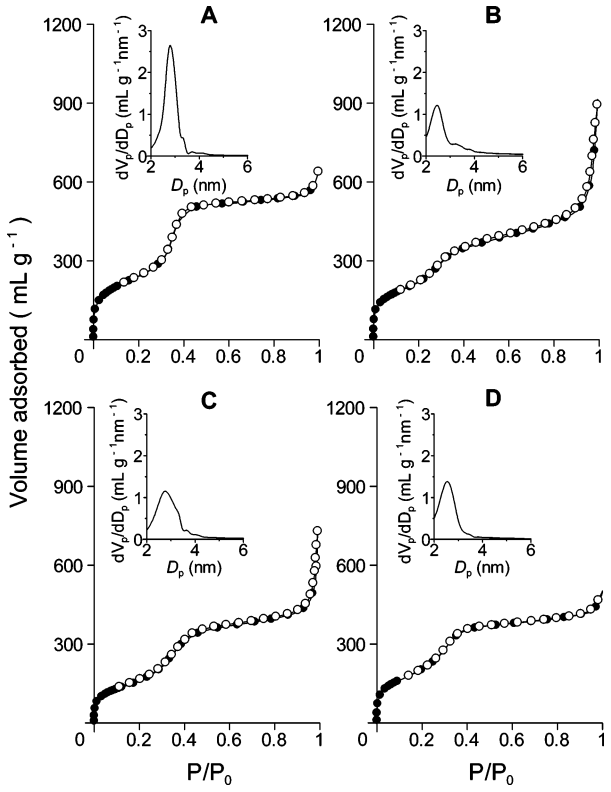

Figure 2. N_2 adsorption (closed symbol) and desorption (open symbol) isotherm and pore size distribution (inset) of (A) V∝HMS-A, (B) V∝HMS-B, (C) V∝HMS-C, and (D) V/HMS catalysts.

Photocatalytic activities of the catalysts were tested by photooxidation of cyclohexane with molecular oxygen (O_2),[9,21] in a conventional liquid/solid system (λ > 300 nm; 5 h) using acetonitrile as a solvent. Without H_2O (Table 1), all four catalysts gave cyclohexanone and cyclohexanol as the main products with a minor amount of CO_2, with V∝HMS-C showing the highest activity. With H_2O, V∝HMS-C maintains catalytic activity, although at reduced level, while other three catalysts completely lose activity. These findings clearly indicate that V∝HMS-C is active even with H_2O. Turnover number (TON) for cyclohexanone and cyclohexanol production [=(cyclohexanone and cyclohexanol formed)/(V amount on catalyst)] is estimated as 1.03 (V∝HMS-A), 1.07 (V∝HMS-B), 2.11 (V∝HMS-C), and 1.07 (V/ HMS) in the absence of water.

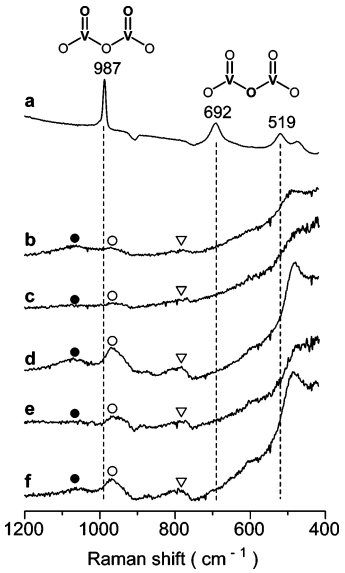

Figure 3. Raman spectra of (a) V_2O_5, (b) V∝HMS-A, (c) V∝HMS-B, (d) V∝HMS-C, (e) V/HMS, and (f) silicious HMS. (Closed circle, Si−O^-; open circle, Si−OH; open triangle, Si−O−Si).

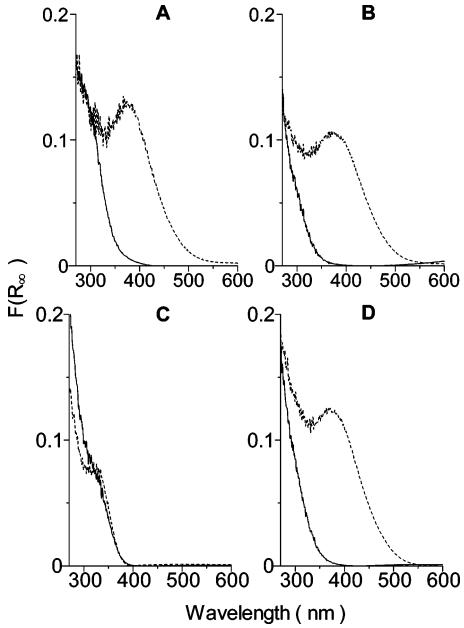

Figure 4. Diffuse reflectance UV−vis spectra of (A) V∝HMS-A, (B) V∝HMS-B, (C) V∝HMS-C, and (D) V/HMS (100 mg), when measured (solid line) after dehydration at 673 K for 2 h and (dotted line) with H_2O (0.3 μmol).

V∝HMS-C, when used with water, shows TON 1.70, indicating that the catalyst is photocatalytically active even with water. When monolayer adsorption capacities of H_2O for all four catalysts were determined,[32] similar values were obtained [1.24 molecules nm^{-2} (V∝HMS-A), 1.40 (V∝HMS-B), 1.46 (V∝HMS-C), and 1.46 (V/HMS)]. This implies that the water-resistant catalytic activity of the V^VO_4 species on V∝HMS-C is derived not from the surface property of the catalysts but from the property of the V^VO_4 species themselves or the local environment around them.

3.2. Properties of VO_4 Species. As shown in Figures 4A, 4B, and 4D (dotted lines), addition of H_2O to V∝HMS-A, V∝HMS-B, and V/HMS catalysts shows distinctive red-shifted absorption centered at 380 nm assigned to octahedrally coordinated V-oxide species, which are formed by H_2O coordination to the V^VO_4 species associated with a V−O bond cleavage

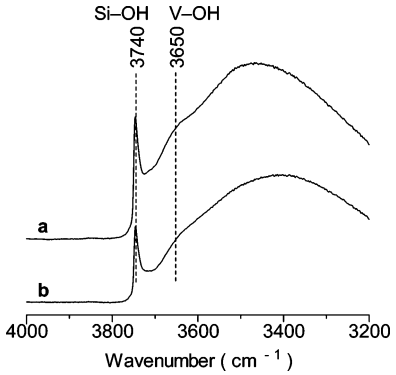

Figure 5. IR spectra of (a) V∝HMS-A and (b) V∝HMS-C, measured after the samples were left in air at room temperature for 3 h.

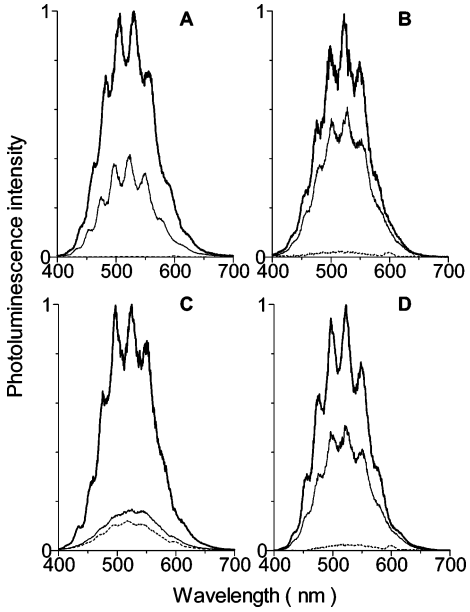

Figure 6. Photoluminescence spectra (λ_{ex} = 250 nm; 77 K) of (A) V∝HMS-A, (B) V∝HMS-B, (C) V∝HMS-C, and (D) V/HMS catalysts (100 mg), when measured (bold line) after dehydration at 673 K for 2 h, (dotted line) with H_2O (0.3 μmol), and (solid line) with cyclohexane (0.3 μmol).

(Scheme 1).[15,28,33] However, as shown in Figure 4C, V∝HMS-C does not show any spectrum change, even with H_2O. IR spectra of V∝HMS-A, V∝HMS-B, and V/HMS measured with H_2O show distinctive V−OH absorption (3650 cm^{-1}),[34] while V∝HMS-C shows only weak absorption (Figure 5: V∝HMS-A and -C, for example). These suggest that the V^VO_4 species on V∝HMS-C may be situated at a site inaccessible by H_2O and/or be stable against hydrolysis.

Figure 6 (bold line) shows photoluminescence spectra of the catalysts (100 mg), when measured in vacuo at 77 K (λ_{ex} = 250 nm). All four catalysts exhibit distinctive luminescence with a vibrational fine structure, attributable to a radiative decay of the photoexcited V^VO_4 species ($V^{IV}O_4$*) formed by photoinduced electron transfer from terminal oxygen (O_T) to V^V center (Scheme 1).[35,36] As shown by dotted lines in Figures 6A, 6B, and 6D, H_2O addition (0.3 μmol) to V∝HMS-A, V∝HMS-B, and V/HMS catalysts leads to a significant decrease in the luminescence intensity (>97%), owing to acceleration of the $V^{IV}O_4$* deactivation (Scheme 1).[37] However, as shown in Figure 6C, V∝HMS-C still shows luminescence even with H_2O (although with 88% decrease in intensity), indicating that interaction between the $V^{IV}O_4$* species and H_2O on V∝HMS-C is weaker than that on the other catalysts.

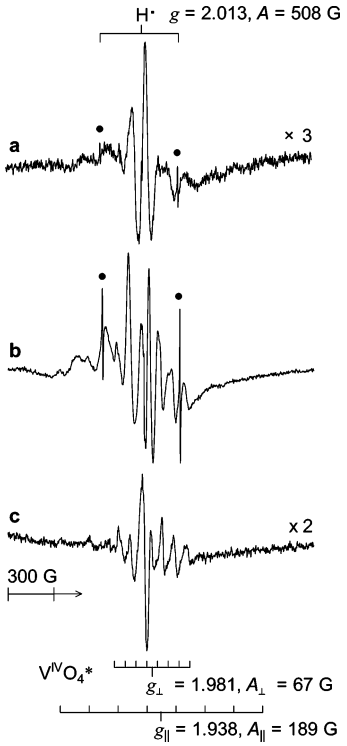

Figure 7. ESR spectra (77 K) of (a) V∝HMS-A and (b) V∝HMS-C obtained with photoirradiation in the presence of H_2 (0.3 μmol) and of (c) V∝HMS-C obtained with photoirradiation in the presence of cyclohexane (0.3 μmol).

As shown in Figure 7a and b (V∝HMS-A and −C, for example), ESR spectra (77 K) of all four catalysts (100 mg) obtained by photoirradiation with H_2 (0.3 μmol) show axially symmetrical hyperfine signals of $V^{IV}O_4$* species ($g_{||}$ = 1.938, $g_\perp$ = 1.981, $A_{||}$ = 189 G, $A_\perp$ = 67 G), along with two sharp signals assigned to hydrogen ($H^\bullet$) radicals (g = 2.013, A = 508 G) formed by a H−H bond cleavage on O_T of the $V^{IV}O_4$* species.[13,38] This indicates that H_2 is accessible to $V^{IV}O_4$* species on all four catalysts. As shown in Figures 8a and 8b, photoirradiation to V∝HMS-A with O_2 (0.3 μmol) gives complicated ESR signals with a hyperfine structure, assigned to oxygen radicals ($O_2^{\bullet-}$ and $O_3^{\bullet-}$),[22,24] which interact with $V^{IV}O_4$*.[39−41] In contrast, as shown in Figure 8c, V∝HMS-C shows only $V^{IV}O_4$* signal, where signals assigned to oxygen radical do not appear. The results clearly indicate that the $V^{IV}O_4$* species on V∝HMS-C are accessible only by H_2, while the $V^{IV}O_4$* species on the other catalysts are accessible by both H_2 and O_2.

3.3. Different VO_4 Structure. The distinct properties of V∝HMS-C catalyst can be explained by different V^VO_4 species derived from the synthesis methods. In the case of V/HMS synthesis, V species are impregnated on silica surface, thus resulting in the formation of *exposed* V^VO_4 species anchored on a silica surface (Scheme 2c).[36,42] In the case of V∝HMS-A synthesis, surfactant DA is added to an aqueous Na_3VO_4 solution at first; hence, the formed DA micelle is surrounded by V species. Upon subsequent TEOS addition, the V-adsorbed micelle is then surrounded by Si species (Scheme 2a); calcination of the resulting gel therefore also leads to a formation of *exposed* V^VO_4 species on the pore wall of HMS (Scheme 2c). In the case of V∝HMS-B synthesis, water containing DA is added to a mixture of $VOSO_4$ and TEOS, thus promoting a simultaneous hydrolysis of both precursors and adsorption of Si and V species around the surfactant micelle. The rate of $VOSO_4$ hydrolysis is, however, higher than that of TEOS,[43,44] such that V species surround the surfactant micelle more rapidly

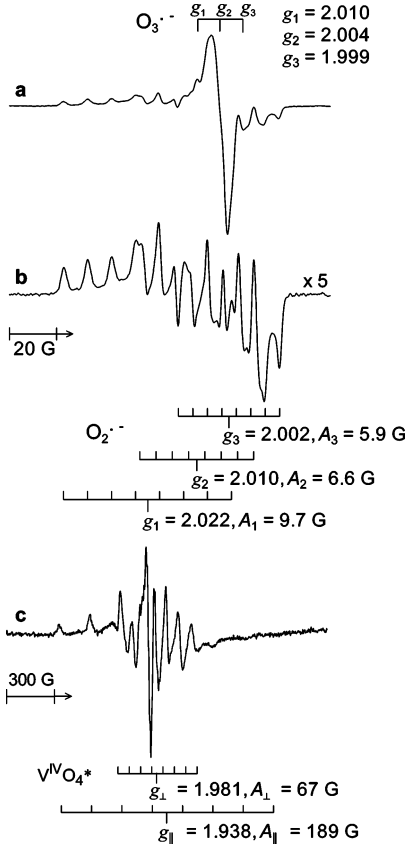

Figure 8. ESR spectra (77 K) of V∝HMS-A (100 mg) obtained (a) with photoirradiation in the presence of O_2 (0.3 μmol), (b) followed by letting it stand at room temperature for 3 min, and of (c) V∝HMS-C obtained with photoirradiation in the presence of O_2 (0.3 μmol). The disappearance of $O_3^{\bullet-}$ signal on spectrum (b) is because $O_3^{\bullet-}$ is unstable at room temperature, while $O_2^{\bullet-}$ is stable.[22,24]

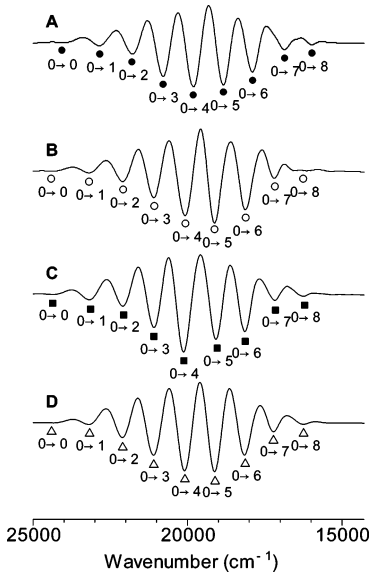

Figure 9. Second derivative of photoluminescence spectra of (A) V∝HMS-A, (B) V∝HMS-B, (C) V∝HMS-C, and (D) V/HMS, measured after dehydration in vacuo at 673 K for 2 h. Symbols in the figure denote vibrational transitions of the respective VO_4 species.

(Scheme 2a). As a result of this, V^VO_4 species still form the *exposed* structure on the surface of HMS pore (Scheme 2c). In contrast, for V∝HMS-C synthesis, water is added to a mixture of Na_3VO_4 and TEOS first; this leads to a partial hydrolysis of V and Si species, forming a pre-network gel that arranges V and Si species homogeneously. Subsequent DA addition leads to a surrounding of the micelle by the gel, thus promoting homogeneous adsorption of V and Si species around the surfactant micelle (Scheme 2b). This probably promotes a formation of V^VO_4 species *confined* within silica matrix, as shown in Scheme 2d. As shown in Table 1, total V contents of all four catalysts, determined by ICP-AES analysis, are similar. However, V content of V∝HMS-C determined by a X-ray fluorescence spectrometer[45] is much lower (<34%) than that of the other catalysts. This may be because of a fluorescence scattering by silica layer.[46] This finding supports the confined V^VO_4 structure on V∝HMS-C.

The confined V^VO_4 structure on V∝HMS-C is also confirmed by second derivatization of the photoluminescence spectra of the respective catalysts (Figure 9). Each spectrum obtained consists of only one emitting species, indicating that each catalyst contains single V^VO_4 species. Table 2 summarizes vibrational energies of the V═O bond of V^VO_4 on the respective

SCHEME 2

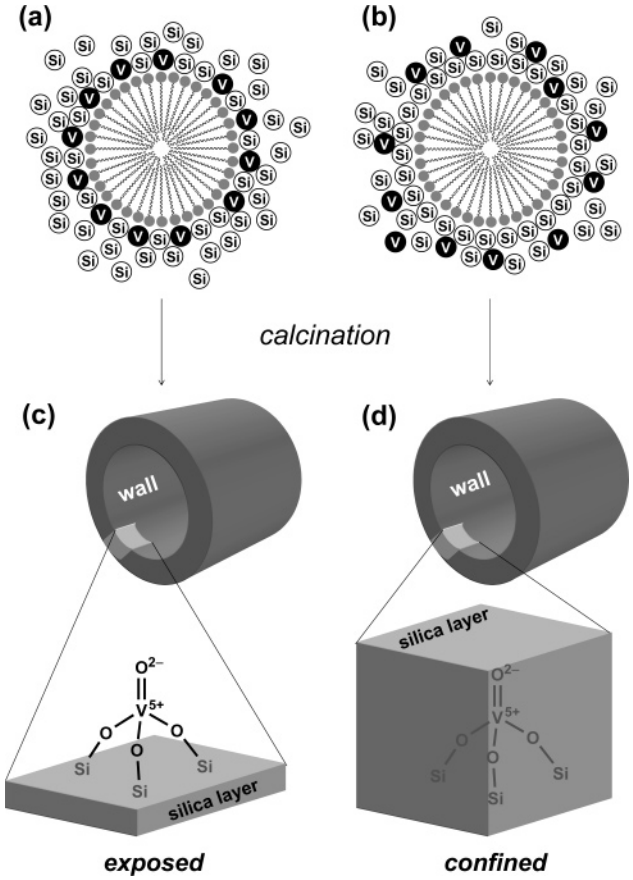

TABLE 2: Properties of VO_4 Species on Respective Catalysts

catalyst	V═O vibrational energy (cm^{-1})	V═O bond length[a] (Å)	percentage of confined VO_4 species[b] (%)	τ_{lum}(77 K) (ms)
V∝HMS-A	1029	1.568	5.5	20.5
V∝HMS-B	991	1.611	13.0	17.0
V∝HMS-C	1054	1.539	84.9	27.5
V/HMS	1013	1.586	15.5	17.5

[a] V═O bond length (Å) = 2.751−0.00115 × V═O vibrational energy (cm^{-1}) (ref 47). [b] The percentage of VO_4 species remaining on the catalysts when washing with an aqueous NH_3OAc (1 M) solution at room temperature for 12 h.

catalysts, calculated from the transition between (0→0) and (0→1), and V═O bond length of the species.[47] The V═O lengths for V^VO_4 on respective catalysts are estimated to be 1.568 Å (V∝HMS-A), 1.611 (V∝HMS-B), 1.539 (V∝HMS-C), and 1.586 (V/HMS), indicating that V^VO_4 species on V∝HMS-C have the shortest V═O length among the catalysts. This suggests that V^VO_4 species on V∝HMS-C have a more distorted structure than on the other catalysts.[47−52] This is probably because of the confinement of the V^VO_4 species by silica layer (Scheme 2d). The result again supports the confined V^VO_4 structure on V∝HMS-C. As described previously,[53−55] treatment of V-containing silica with an ammonium acetate (NH_3OAc) solution leads to removal of the extralattice V-oxide species. When all four catalysts were stirred in an aqueous NH_3-OAc solution (1 M) at room temperature for 12 h, percentage removal of the V^VO_4 species from the catalysts was estimated to be 94.5 (V∝HMS-A), 87.0 (V∝HMS-B), 15.1 (V∝HMS-C), and 84.5 (V/HMS), respectively. The results indicate that most of the V^VO_4 species on V∝HMS-C does not exist on the extralattice, while the V^VO_4 species on the other catalysts do (Table 2). This finding again supports the confined structure of the V^VO_4 species on V∝HMS-C, while the species on other catalysts have exposed structure (Schemes 2c and 2d).

Based on the above findings, different activities of the catalysts toward H_2, O_2, and H_2O are therefore explained as follows: on V∝HMS-A, V∝HMS-B, and V/HMS catalysts, both H_2 and O_2 access easily the exposed $V^{IV}O_4$* species, thus producing the corresponding radicals (Figures 7a, 8a, and 8b). On the confined $V^{IV}O_4$* of V∝HMS-C, small H_2 molecule (2.89 Å)[56,57] can pass through the silica layer and access $V^{IV}O_4$*, thus producing $H^•$ radical (Figure 7b). Larger O_2 (3.46 Å),[56] however, cannot access the confined $V^{IV}O_4$*, resulting in no radical production (Figure 8c). H_2O has much smaller size (2.65 Å),[56] implying that H_2O can access the confined $V^{IV}O_4$*. As shown in Figure 6C, photoluminescence of $V^{IV}O_4$* is quenched by the addition of H_2O, indicating that the confined $V^{IV}O_4$* is actually accessible by H_2O. However, as shown in Figure 4C, hydrolysis of V^VO_4 on V∝HMS-C does not occur. This may be because the V^VO_4 species on V∝HMS-C is stabilized by the confinement within silica layer. V∝HMS-A, V∝HMS-B, and V/HMS catalysts, when recovered following photocatalytic reaction with H_2O (Table 1), show ca. 5% decrease in V content, indicating that V leaching takes place on these catalysts. V∝HMS-C, however, does not show any decrease in V content. The results indicate that the confinement of V^VO_4 by the silica layer suppresses the hydrolysis and leaching of the species.

3.4. Photocatalytic Mechanism. Cyclohexane, with large size (6 Å),[56] cannot pass through the silica layer. However, as shown by a solid line in Figure 6C, photoluminescence intensity of V∝HMS-C, when measured with cyclohexane (0.3 μmol), is 83% weaker than that obtained in vacuo (bold line). This indicates that cyclohexane can interact with the confined $V^{IV}O_4$*, despite its large size. ESR measurement of V∝HMS-C, with photoirradiation in the presence of cyclohexane (0.3 μmol) at 77 K, shows only $V^{IV}O_4$* signal (Figure 7c), where a signal assigned to cyclohexanyl radical[58] does not appear. The O_T on $V^{IV}O_4$*, formed by photoinduced electron transfer, has electrophilic character.[59] The decrease in the photoluminescence intensity of $V^{IV}O_4$* in the presence of cyclohexane (Figure 6C) may be attributable to a formation of [cyclohexane-O_T] complex, via a proton attraction by the electrophilic O_T.[21,59] Due to the large size of cyclohexane, this complex may form *through* the silica layer, where a proton of cyclohexane plunges into the layer, as shown in Scheme 3.[57] Cyclohexanone oxidation may

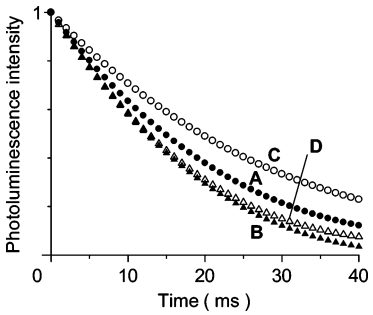

Figure 10. Photoluminescence decays (λ_{ex} = 250 nm; 77 K) of (A) V∝HMS-A (λ_{em} = 507 nm), (B) V∝HMS-B (λ_{em} = 498 nm), (C) V∝HMS-C (λ_{em} = 497 nm), and (D) V/HMS (λ_{em} = 497 nm) catalysts, when measured after dehydration at 673 K for 2 h. The detection wavelengths correspond to the maximum emission wavelength of the respective catalysts.

SCHEME 3

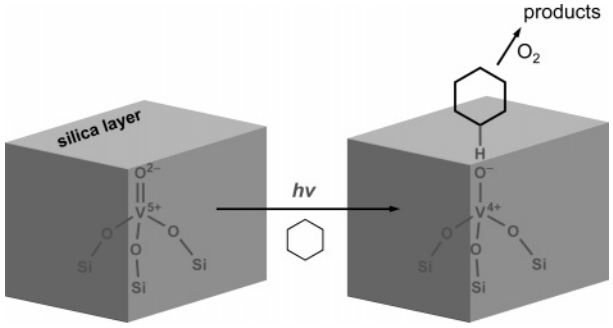

proceed via a reaction of this complex with O_2 (Scheme 3). To check this scheme, the following two experiments were carried out:[21] (i) photoirradiation to V∝HMS-C with cyclohexane followed by addition of O_2 while stopping photoirradiation;[60] and (ii) photoirradiation to V∝HMS-C with O_2 followed by addition of cyclohexane while stopping photoirradiation.[61] Only the former procedure promoted cyclohexane oxidation. The results strongly support the proposed reaction mechanism (Scheme 3).

A notable feature of the V∝HMS-C catalyst is the higher photocatalytic activity than that of V∝HMS-A, V∝HMS-B, and V/HMS catalysts even without H_2O (Table 1), although access of cyclohexane to the confined $V^{IV}O_4$* species would seem to be difficult. As shown in Figure 6 (solid line), photoluminescence intensity of $V^{IV}O_4$* on all four catalysts decreases with the addition of cyclohexane. The decrease in the intensity on V∝HMS-C to the intensity obtained without cyclohexane is estimated to be 83%, whereas other catalysts show a lower decrease: 58% (V∝HMS-A), 39% (V∝HMS-B), and 49% (V/HMS). This indicates that the confined $V^{IV}O_4$* species on V∝HMS-C is quenched easily despite its restricted structure. As described above and shown in Scheme 3, $V^{IV}O_4$* species is quenched by cyclohexane via a proton attraction by the electrophilic O_T. The strong attraction of cyclohexane by $V^{IV}O_4$* on V∝HMS-C is likely to be attributable to high electrophilicity of O_T, probably owing to strong distortion of the $V^{IV}O_4$* species. Relatively higher photocatalytic activity of the distorted $V^{IV}O_4$* species was observed for NO decomposition.[51,52] Figure 10 shows results of time-resolved photoluminescent measurement of the catalysts in vacuo at 77 K (λ_{ex} = 250 nm). The luminescence lifetime of $V^{IV}O_4$* on V∝HMS-C is determined to be 27.5 ms, while the other catalysts show much shorter lifetime (<21 ms), as summarized in Table 2. The longer lifetime of $V^{IV}O_4$* on V∝HMS-C is attributable to their distorted

structure.[48−52] The above findings indicate that the higher photocatalytic activity of V∝HMS-C is attributable to the higher electrophilicity of O_T and the longer lifetime of the distorted $V^{IV}O_4$* species, derived from the confined structure. The results presented here demonstrate that a slight modification to the conventional surfactant-templating method creates a HMS catalyst containing the confined V^VO_4 species with high photocatalytic activity and stability against water. The results provide important and useful insight into the development of more efficient V-based photocatalysts. We are now applying this method to the synthesis of HMS catalysts containing other metal-oxide species with confined structure.

4. Conclusion

Vanadium-containing mesoporous silica molecular sieve (V∝HMS) with highly dispersed and tetrahedrally coordinated V-oxide species (V^VO_4) has been prepared by a modified surfactant-templating method. Photocatalytic activity and stability of the catalyst have been studied, with the following results:

(1) The catalyst (V∝HMS-C), prepared by a modified templating method consisting of an addition of surfactant to a mixture of water, alcohol, and Si and V precursors followed by calcination, shows high photocatalytic activity even with water. Other V-containing HMS catalysts prepared by conventional templating methods or impregnation method show almost no activity with water due to hydrolysis of the V^VO_4 species, while V∝HMS-C does not show hydrolysis of the species.

(2) ESR and photoluminescence measurements reveal that the V^VO_4 species formed on V∝HMS-C have a structure that are confined within a silica layer, while other catalysts contain V^VO_4 species exposed on the surface of the catalysts. The confinement stabilizes the V^VO_4 species, thus suppressing the hydrolysis of the species. V leaching during photoreaction with water does not take place, which may allow the catalyst to be recycled for further reaction.

(3) The confined V^VO_4 on V∝HMS-C demonstrates higher photocatalytic activity than the other catalysts, despite its confined structure. Photoluminescence quenching and time-resolved luminescence measurements reveal that the excited state of the V^VO_4 species ($V^{IV}O_4$*) has a terminal oxygen of high electrophilicity and has a long lifetime, derived from their confined structure, which lead to the high photocatalytic activity.

Acknowledgment. We are thankful for financial support by the Grant-in-Aid for Scientific Research (No. 15360430) and the Grant-in-Aid for Scientific Research on Priority Areas (417) "Fundamental Science and Technology of Photofunctional Interfaces" (Nos. 15033244 and 17029037) from the Ministry of Education, Culture, Sports, Science and Technology, Japan (MEXT). We are also grateful to the Division of Chemical Engineering for the Lend-Lease Laboratory System and Mr. Suguru Ota for his experimental assistance.

References and Notes

(1) Maldotti, A.; Molinari, A.; Amadelli, R. *Chem. Rev.* **2002**, *102*, 3811.

(2) Anpo, M. *Photofunctional Zeolites*; Nova Science Publishers Inc: New York, 2000.

(3) Matsuoka, M.; Anpo, M. *J. Photochem. Photobiol. C* **2003**, *3*, 225.

(4) Yoshida, H.; Murata, C.; Hattori, T. *J. Catal.* **2000**, *194*, 364.

(5) Tanaka, T.; Nishimura, Y.; Kawasaki, S.; Funabiki, T.; Yoshida, S. *J. Chem. Soc., Chem. Commun.* **1987**, 506.

(6) Tran, K.; Hanning-Lee, M. A.; Biswas, A.; Stiegman, A. E.; Scott, G. W. *J. Am. Chem. Soc.* **1995**, *117*, 2618.

(7) Zhang, S. G.; Higashimoto, S.; Yamashita, H.; Anpo, M. *J. Phys. Chem. B* **1998**, *102*, 5590.

(8) Tanaka, T.; Ito, T.; Takenaka, S.; Funabiki, T.; Yoshida, S. *Catal. Today* **2000**, *61*, 109.

(9) Teramura, K.; Tanaka, T.; Yamamoto, T.; Funabiki, T. *J. Mol Catal. A* **2001**, *165*, 299.

(10) Yoshida, S.; Magatani, Y.; Noda, S.; Funabiki, T. *J. Chem. Soc., Chem. Commun.* **1981**, 601.

(11) Tanaka, T.; Ooe, M.; Funabiki, T.; Yoshida, S. *J. Chem. Soc., Faraday Trans. 1* **1986**, *82*, 35.

(12) Amano, F.; Tanaka, T.; Funabiki, T. *Langmuir* **2004**, *20*, 4236.

(13) Anpo, M.; Zhang, S. G.; Higashimoto, S.; Matsuoka, M.; Yamashita, H.; Ichihashi, Y.; Matsumura, Y.; Souma, Y. *J. Phys. Chem. B* **1999**, *103*, 9295.

(14) Zhang, S. G.; Ariyuki, M.; Mishima, H.; Higashimoto, S.; Yamashita, H.; Anpo, M. *Microporous Mesoporous Mater.* **1998**, *21*, 621.

(15) Narayana, M.; Narasimhan, C. S.; Kevan, L. *J. Catal.* **1983**, *79*, 237.

(16) Tanaka, T.; Yamashita, H.; Tsuchitani, R.; Funabiki, T.; Yoshida, S. *J. Chem. Soc., Faraday Trans. 1* **1988**, *84*, 2987.

(17) Gontier, S.; Tuel, A. *Microporous Mater.* **1995**, *5*, 161.

(18) Reddy, J. S.; Liu, P.; Sayari, A. *Appl. Catal. A* **1996**, *148*, 7.

(19) Deng, Y.; Lettmann, C.; Maier, W. F. *Appl. Catal. A* **2001**, *214*, 31.

(20) Zhang, W.; Wang, J.; Tanev, P. T.; Pinnavaia, T. J. *Chem. Commun.* **1996**, 979.

(21) Shiraishi, Y.; Teshima, Y.; Hirai, T. *Chem. Commun.* **2005**, 4569.

(22) Shiraishi, Y.; Saito, N.; Hirai, T. *J. Am. Chem. Soc.* **2005**, *127*, 8304.

(23) Shiraishi, Y.; Saito, N.; Hirai, T. *J. Am. Chem. Soc.* **2005**, *127*, 12820.

(24) Shiraishi, Y.; Morishita, M.; Hirai, T. *Chem. Commun.* **2005**, 5977.

(25) Shiraishi, Y.; Koizumi, H.; Hirai, T. *J. Phys. Chem. B* **2005**, *109*, 8580.

(26) Shiraishi, Y.; Kohno, Y.; Hirai, T. *J. Phys. Chem. B* **2005**, *109*, 19139.

(27) Gao, X.; Bare, S. R.; Fierro, J. L. G.; Banares, M. A.; Wachs, I. E. *J. Phys. Chem. B* **1998**, *102*, 5653.

(28) Kornatowski, J.; Sychev, M.; Kuzenkov, S.; Strnadová, K.; Pilz, W.; Kassner, D.; Pieper, G.; Baur, W. H. *J. Chem. Soc., Faraday Trans.* **1995**, *91*, 2217.

(29) Kornatowski, J.; Wichterlová, B.; Jirkovsk×c6, J.; Löffler, E.; Pilz, W. *J. Chem. Soc., Faraday Trans.* **1996**, *92*, 1067.

(30) Das, N.; Eckert, H.; Hu, H.; Wachs, I. E.; Walzer, J. F.; Feher, F. J. *J. Phys. Chem.* **1993**, *97*, 8240.

(31) Chao, K. J.; Wu, C. N.; Chang, H.; Lee, L. J.; Hu, S.-f. *J. Phys. Chem. B* **1997**, *101*, 6341.

(32) The monolayer adsorption amounts of H_2O on the catalysts were measured using the apparatus employed for N_2 adsorption−desorption measurement. The values for monolayer adsorption capacity were determined by dividing the amount of H_2O adsorbed on the catalysts by the BET surface area of the catalysts: Miura, K.; Morimoto, T. *Langmuir* **1994**, *10*, 807.

(33) Dzwigaj, S.; Matsuoka, M.; Franck, R.; Anpo, M.; Che, M. *J. Phys. Chem. B* **1998**, *102*, 6309.

(34) Dzwigaj, S.; Massiani, P.; Davidson, A.; Che, M. *J. Mol. Catal. A* **2000**, *155*, 169.

(35) Anpo, M.; Tanahashi, I.; Kubokawa, Y. *J. Phys. Chem.* **1980**, *84*, 3440.

(36) Anpo, M.; Sunamoto, M.; Che, M. *J. Phys. Chem.* **1989**, *93*, 1187.

(37) Dzwigaj, S.; Krafft, J.-M.; Che, M.; Lim, S.; Haller, G. L. *J. Phys. Chem. B* **2003**, *107*, 3856.

(38) Wall, L. A.; Brown, D. W.; Florin, R. E. *J. Phys. Chem.* **1959**, *63*, 1762.

(39) Shvets, V. A.; Vorotinzev, V. M.; Kazansky, V. B. *J. Catal.* **1969**, *15*, 214.

(40) Che, M.; Tench, A. J. *Adv. Catal.* **1983**, *32*, 1.

(41) Shvets, V. A.; Kazansky, V. B. *J. Catal.* **1972**, *25*, 123.

(42) Patterson, H. H.; Cheng, J.; Despres, S.; Sunamoto, M.; Anpo, M. *J. Phys. Chem.* **1991**, *95*, 8813.

(43) Hüsing, N.; Launay, B.; Doshi, D.; Kickelbick, G. *Chem. Mater.* **2002**, *14*, 2429.

(44) Brinker, C. J.; Scherer, G. W. *Sol−Gel Science*; Academic Press: New York, 1990.

(45) Measured on an energy-dispersive XRF spectrometer (Seiko Instruments, Inc.; SEA2110), operated at 50 kV and 850 mA, equipped with a solid-state detector, where the Kα line of V (4.950 eV) was used for measurement.

(46) Guo, J.; Skytt, P.; Wassdahl, N.; Nordgren, J. *J. Electron. Spectrosc.* **2000**, *110*, 41.

(47) Iwamoto, M.; Furukawa, H.; Matsukami, K.; Takenaka, T.; Kagawa, S. *J. Am. Chem. Soc.* **1983**, *105*, 3719.

(48) Dzwigaj, S.; Matsuoka, M.; Anpo, M.; Che, M. *J. Phys. Chem. B* **2000**, *104*, 6012.

(49) Dzwigaj, S.; Matsuoka, M.; Anpo, M.; Che, M. *Catal. Lett.* **2001**, *72*, 211.

(50) Anpo, M.; Higashimoto, S.; Matsuoka, M.; Zhanpeisov, N.; Shioya, Y.; Dzwigaj, S.; Che, M. *Catal. Today* **2003**, *78*, 211.

(51) Dzwigaj, S. *Curr. Opin. Solid State Mater. Sci.* **2003**, *7*, 461.

(52) Dzwigaj, S.; Matsuoka, M.; Anpo, M.; Che, M. *Res. Chem. Intermed.* **2003**, *29*, 665.

(53) Centi, G.; Parathoner, S.; Trifiró, F.; Aboukais, A.; Aïssi, C. F.; Guelton, M. *J. Phys. Chem.* **1992**, *96*, 2617.

(54) Sen, T.; Ramaswamy, V.; Ganapathy, S.; Rajamohanan, P. R.; Sivasanker, S. *J. Phys. Chem.* **1996**, *100*, 3809.

(55) Sen, T.; Rajamohanan, P. R.; Ganapathy, S.; Sivasanker, S. *J. Catal.* **1996**, *163*, 354.

(56) Breck,D. W. *Zeolite Molecular Sieves, Structure, Chemistry, and Use*; Wiley: New York, 1974.

(57) Oyama, S. T.; Lee, D.; Hacarlioglu, P.; Saraf, R. F. *J. Membr. Sci.* **2004**, *244*, 45.

(58) Ohmae, T.; Ohnishi, S.; Kuwata, K.; Sakurai, H.; Nitta, I. *Bull. Chem. Soc. Jpn.* **1967**, *40*, 226.

(59) Wada, K.; Yamada, H.; Watanabe, Y.; Mitsudo, T. *J. Chem. Soc., Faraday Trans.* **1998**, *94*, 1771.

(60) Reaction was performed within a conventional closed system (capacity, 6 cm^3) (ref 21). V∝HMS-C (50 mg) was spread on the flat bottom (2 cm^2) of the quartz vessel and the vessel was evacuated at room temperature. Cyclohexane (0.5 mmol) was introduced to the vessel, and the sample was photoirradiated in a static condition. After photoirradiation (5 h), the vessel was immediately filled with O_2 (1 atm) and left for 5 min. Acetonitrile (5 mL) was added to the vessel, and the catalyst was rinsed well by ultrasonication for 5 min. The resulting solution was recovered by centrifugation and then analyzed. The yields of cyclohexanone and cyclohexanol were 0.32 and 0.27 μmol, respectively.

(61) V∝HMS-C (50 mg) was spread on the quartz vessel (ref 60), which was evacuated at room temperature. O_2 (200 Torr) was introduced to the vessel and photoirradiated for 5 h. After photoirradiation, cyclohexane (260 Torr; 80 μmol) was immediately introduced to the vessel, and the vessel was left for 5 min. Catalyst was rinsed with acetonitrile (5 mL), and the solution was recovered by centrifugation. None of the products were detected by GC analysis.